Magmatic inflation at a dormant stratovolcano: 1996–1998 activity at Mount Peulik volcano, Alaska, revealed by satellite radar interferometry

Zhong Lu,[1] Charles Wicks Jr.,[2] Daniel Dzurisin,[3] John A. Power,[4] Seth C. Moran,[4] and Wayne Thatcher[2]

[1] A series of ERS radar interferograms that collectively span the time interval from July 1992 to August 2000 reveal that a presumed magma body located 6.6 ± 0.5 km beneath the southwest flank of the Mount Peulik volcano inflated 0.051 ± 0.005 km^3 between October 1996 and September 1998. Peulik has been active only twice during historical time, in 1814 and 1852, and the volcano was otherwise quiescent during the 1990s. The inflation episode spanned at least several months because separate interferograms show that the associated ground deformation was progressive. The average inflation rate of the magma body was ~0.003 km^3/month from October 1996 to September 1997, peaked at 0.005 km^3/month from 26 June to 9 October 1997, and dropped to ~0.001 km^3/month from October 1997 to September 1998. An intense earthquake swarm, including three M_L 4.8–5.2 events, began on 8 May 1998 near Becharof Lake, ~30 km northwest of Peulik. More than 400 earthquakes with a cumulative moment of 7.15×10^{17} N m were recorded in the area through 19 October 1998. Although the inflation and earthquake swarm occurred at about the same time, the static stress changes that we calculated in the epicentral area due to inflation beneath Peulik appear too small to provide a causal link. The 1996–1998 inflation episode at Peulik confirms that satellite radar interferometry can be used to detect magma accumulation beneath dormant volcanoes at least several months before other signs of unrest are apparent. This application represents a first step toward understanding the eruption cycle at Peulik and other stratovolcanoes with characteristically long repose periods.   *INDEX TERMS:* 1206 Geodesy and Gravity: Crustal movements—interplate (8155); 6924 Radio Science: Interferometry; 6969 Radio Science: Remote sensing; 8419 Volcanology: Eruption monitoring (7280); 8494 Volcanology: Instruments and techniques; *KEYWORDS:* interferometry, synthetic aperture radar (SAR), volcano deformation, earthquake swarm, Peulik, volcano monitoring

1. Introduction

[2] A fundamental challenge facing volcanologists is to anticipate which dormant volcanoes are likely to reawaken next, even though they may have been quiescent for a very long time and may currently exhibit no signs of unusual activity. At such volcanoes, eruptions are rare by human standards, and the associated hazards are generally underappreciated, a situation that invites encroachment by cities and thus increases the likelihood of future disasters. Much progress has been made recently toward relatively short-term eruption prediction on the basis of interpretation of precursory activity (e.g., seismicity, ground deformation, gas emission) that is typically recognized a few days to several months before eruptions [*Swanson et al.*, 1983; *Harlow et al.*, 1997; *Punongbayan et al.*, 1996; *Montserrat Volcano Monitoring Team*, 1997]. On the other hand, the ability to anticipate the onset of such activity has been elusive, except in rare cases where eruptions occur on a somewhat regular timetable. As a result, conventional wisdom holds that dormant volcanoes are essentially inscrutable except during brief periods of precursory activity that mark only the last few kilometers of magma's long rise toward the surface.

[3] To improve this situation, volcanologists require a monitoring tool capable of tracking some aspect of the eruption cycle before the onset of short-term precursors, which typically start when magma is already within a few kilometers of the surface. Such a breakthrough seems feasible because conceptually the eruption cycle is a continuum from deep magma generation through surface eruption, including such intermediate phases as partial

[1]U.S. Geological Survey, EROS Data Center, Raytheon ITSS, Sioux Falls, South Dakota, USA.

[2]U.S. Geological Survey, Menlo Park, California, USA.

[3]U.S. Geological Survey, David A. Johnston Cascades Volcano Observatory, Vancouver, Washington, USA.

[4]U.S. Geological Survey, Alaska Volcano Observatory, Anchorage, Alaska, USA.

melting, initial ascent through the upper mantle and lower crust, crustal assimilation, magma mixing, degassing, shallow storage, and final ascent to the surface. In this context, the absence of measurable precursors until very late in the cycle, when magma begins its final ascent, is an artifact produced mainly by two factors: (1) the brittle-ductile transition typically occurs ~5 km beneath volcanoes, so the slow ascent of magma to that depth is generally not marked by earthquakes [e.g., *Hill*, 1992; *Sibson*, 1982] and (2) most geodetic techniques are not sensitive enough to detect subtle ground deformation that might occur when magma accumulates near or below the brittle-ductile transition, especially if the intrusion occurs episodically in a series of small events or gradually over a long time period.

1.1.   Mapping Volcano Deformation With Interferometric Synthetic Aperture Radar

[4]   The likelihood of progress toward meeting this challenge has increased significantly since the recent advent of volcano monitoring by satellite interferometric synthetic aperture radar (InSAR). The InSAR technique utilizes two or more synthetic aperture radar (SAR) images of the same area acquired at different times to map ground deformation at a horizontal resolution of tens of meters over ~100 km by 100 km areas with centimeter to subcentimeter vertical precision [*Massonnet and Feigl*, 1998]. InSAR is an imaging technique rather than a surveying technique such as the modern Global Positioning System (GPS), so it provides much better spatial coverage that facilitates discovery of subtle deformation patterns that might be missed by relatively scattered sampling in geodetic surveys. Currently, InSAR is not an effective short-term monitoring tool because the orbital repeat times of SAR satellites are long (e.g., 35 days for ERS-2) compared to the typical pace of volcano deformation during the final stages of preeruption unrest. Over periods of months to years, however, InSAR can provide valuable information about volcano deformation with a spatial density that is unobtainable by other geodetic techniques.

[5]   Not surprisingly, InSAR has been quickly and enthusiastically embraced by volcanologists and others interested in volcano deformation, its causes, and implications [e.g., *Massonnet et al.*, 1995; *Vadon and Sigmundsson*, 1996; *Thatcher and Massonnet*, 1997; *Wicks et al.*, 1998; *Zebker et al.*, 2000; *Amelung et al.*, 2000]. Recently, InSAR has been used to study both eruptive and noneruptive processes at several volcanoes in the Aleutian volcanic arc, Alaska. Examples include preeruptive inflation, coeruptive deflation, and posteruptive inflation at Okmok volcano [*Lu et al.*, 2000a]; aseismic inflation at quiescent Westdahl volcano [*Lu et al.*, 2000b]; magmatic intrusion and associated tectonic strain release at Akutan volcano [*Lu et al.*, 2000c]; magmatic intrusion associated with a relatively small eruption in 1995 at Makushin volcano [*Lu et al.*, 2002a]; surface subsidence caused by decreased pore fluid pressure within a shallow hydrothermal system beneath the Kiska volcano [*Lu et al.*, 2002b]; lack of measurable surface deformation associated with "open-system" eruptive activity at Shishaldin volcano [*Lu et al.*, 2000d]; and compaction of young pyroclastic flow deposits at Augustine volcano [*Lu et al.*, 2000d].

1.2.   Mount Peulik Volcano: Setting and Historical Activity

[6]   The Ugashik caldera-Mount Peulik volcanic system, part of the 2500-km-long Aleutian volcanic arc, is located on the Alaska Peninsula ~550 km southwest of Anchorage (Figure 1). Mount Peulik is a small, truncated stratovolcano that partially overlaps the north flank of Ugashik caldera, an island arc collapse caldera, roughly 5 km in diameter, of probable late Pleistocene age [*Miller et al.*, 1998; *Newhall and Dzurisin*, 1988]. There are only two reports of historical activity at Mount Peulik. *Doroshin* [1870, p. 24] stated "...around 1814 its [Peulik] summit collapsed with a rumble, covering the base with enormous boulders." *Miller et al.* [1998] suggested that this report might record an episode of dome destruction. *Doroshin* [1870] also reported that in 1852 he saw only "smoke" coming from the south side of Peulik's summit crater; whether this activity marks a separate eruptive episode is unclear. No fumarolic activity was noted when the summit dome was examined in 1973 [*Miller et al.*, 1998], and no unusual activity of any kind had been noted in the area since the formation of the Ukinrek Maars, ~15 km northwest of Mount Peulik, in 1977.

[7]   The Ukinrek Maars formed during 10 days of phreatomagmatic activity in late March and early April 1977 when basaltic magma intruded near-surface, water-saturated pyroclastic deposits [*Kienle et al.*, 1980; *Self et al.*, 1980]. The eruption was preceded by at least a year of increased earthquake activity in the area. A sparse regional seismic network recorded five locatable events from March 1976 to February 1977. The largest (*M* 4.5) occurred on 6 March 1976. Another 10 earthquakes of *M* 1.0–2.4 were located in the vicinity of Becharof Lake, at depths of 2–12 km, during the first 5 months following the eruption [*Estes*, 1978]. Numerous small earthquakes undoubtedly accompanied the Ukinrek Maars eruption, but these were too small to be located with the regional seismograph network. Two portable short-period seismographs that were operated within 2 km of the vents from 15 to 20 April 1977, just after the eruptions ceased, recorded a high level of local microearthquake activity. Another seismograph located on Gas Rocks, 3 km northeast of the Ukinrek Maars, continued to record sporadic earthquake activity at least through 1979 [*Kienle et al.*, 1980]. Seismic coverage of the Becharof Lake-Mount Peulik area was sporadic and generally poor from 1977 to 1995, with the exception of a 14-station network in Katmai National Park operated from 1987 through the early 1990s [*Ward et al.*, 1991]. With that qualification we believe that there were no swarms during that period comparable to or larger than the 1977 swarm.

1.3.   The 1998 Becharof Lake Earthquake Swarm

[8]   At 0030 UT on 9 May 1998, a M_L 5.2 (local magnitude) earthquake occurred ~30 km northwest of Peulik, near the western shoreline of Becharof Lake (Figure 1). This large event was strongly felt in nearby communities and was followed by a M_L 4.8 event at 0059 UT and a M_L 5.1 event at 0355 UT. An intense swarm of smaller earthquakes ensued, and by 19 October 1998 a total of 414 events had been detected in an area centered
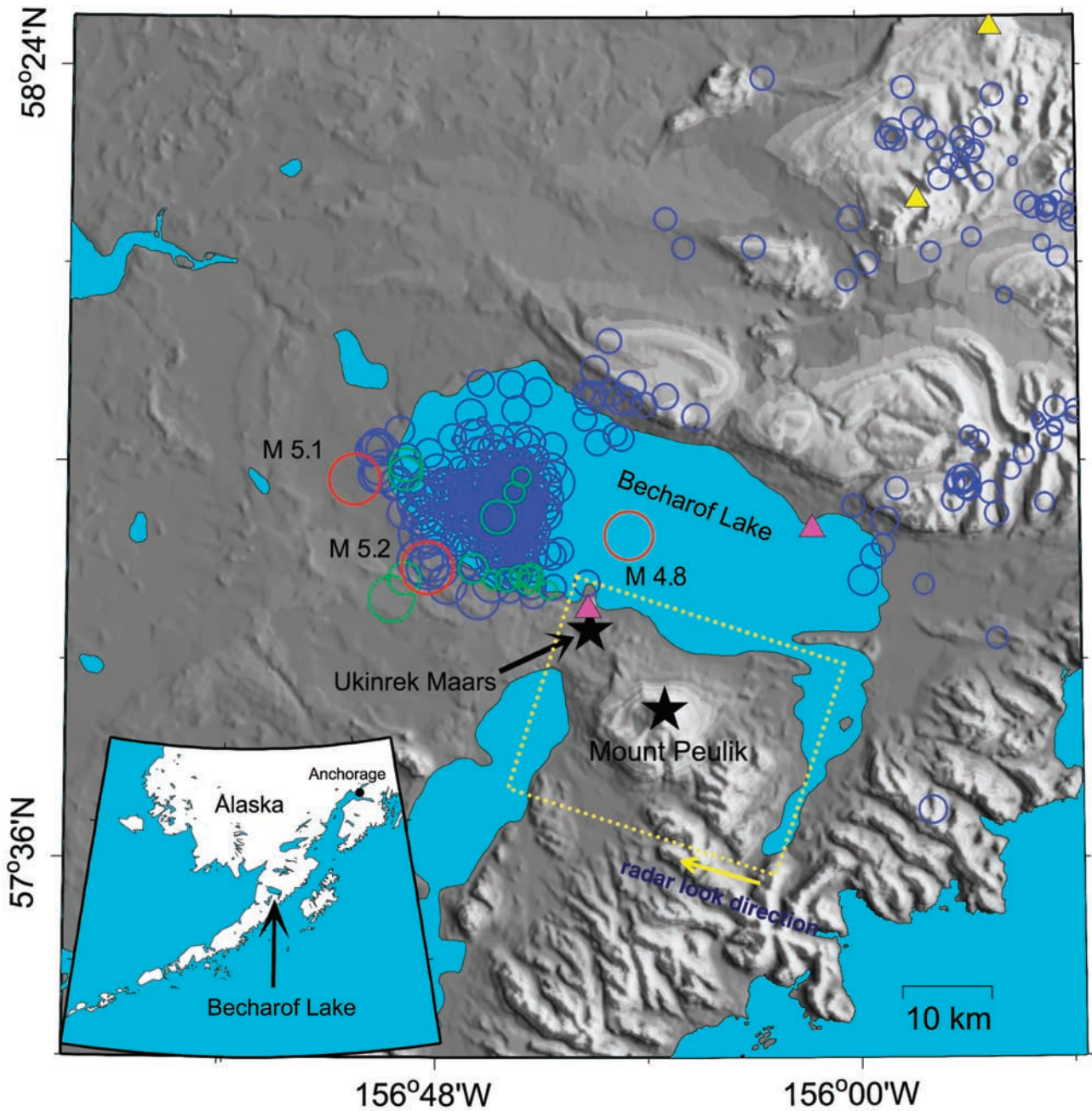
Figure 1. Epicenters for earthquakes in the 1998 Becharof Lake swarm. Red circles show the locations of the three largest events. These three plus all of the earthquakes represented by blue circles occurred from 8 May to 19 October 1998. Green circles represent 15 events located in 1976–1977 by *Estes*, [1978] associated with the 1977 Ukinrek Maars eruption. Black stars represent the Mount Peulik volcano and Ukinrek Maars. Yellow triangles represent the two nearest permanent seismic stations in the Katmai network operated by AVO, and the pink triangles represent two temporary stations deployed between 14 and 16 May 1998. The yellow dashed polygon outlines interferograms shown in Figures 3 and 4.

~30 km northwest of Peulik. The cumulative seismic moment of the swarm was 7.15×10^{17} N m (Figure 2), equivalent to that of a M_w 5.8 earthquake. This compares to 2.7×10^{18} N m for the March 1996 swarm at Akutan Island, which was associated with inflation and shallow dike intrusion beneath Akutan volcano [*Lu et al.*, 2000c].

[9] The nearest seismometers to the study area are located 50–70 km northeast in the Katmai network (Figure 1) and ~125 km southwest in the Aniakchak network, both operated by the Alaska Volcano Observatory (AVO). Since the Katmai network was reactivated in the summer of 1995, the earthquake record for the study area is complete to M_L 2.2, and the uncertainty in epicenter locations is about ±5 km. Most of the earthquakes in the 1998 Becharof Lake swarm were located using only the Katmai network; the Aniakchak network detected P arrivals only from the largest events.
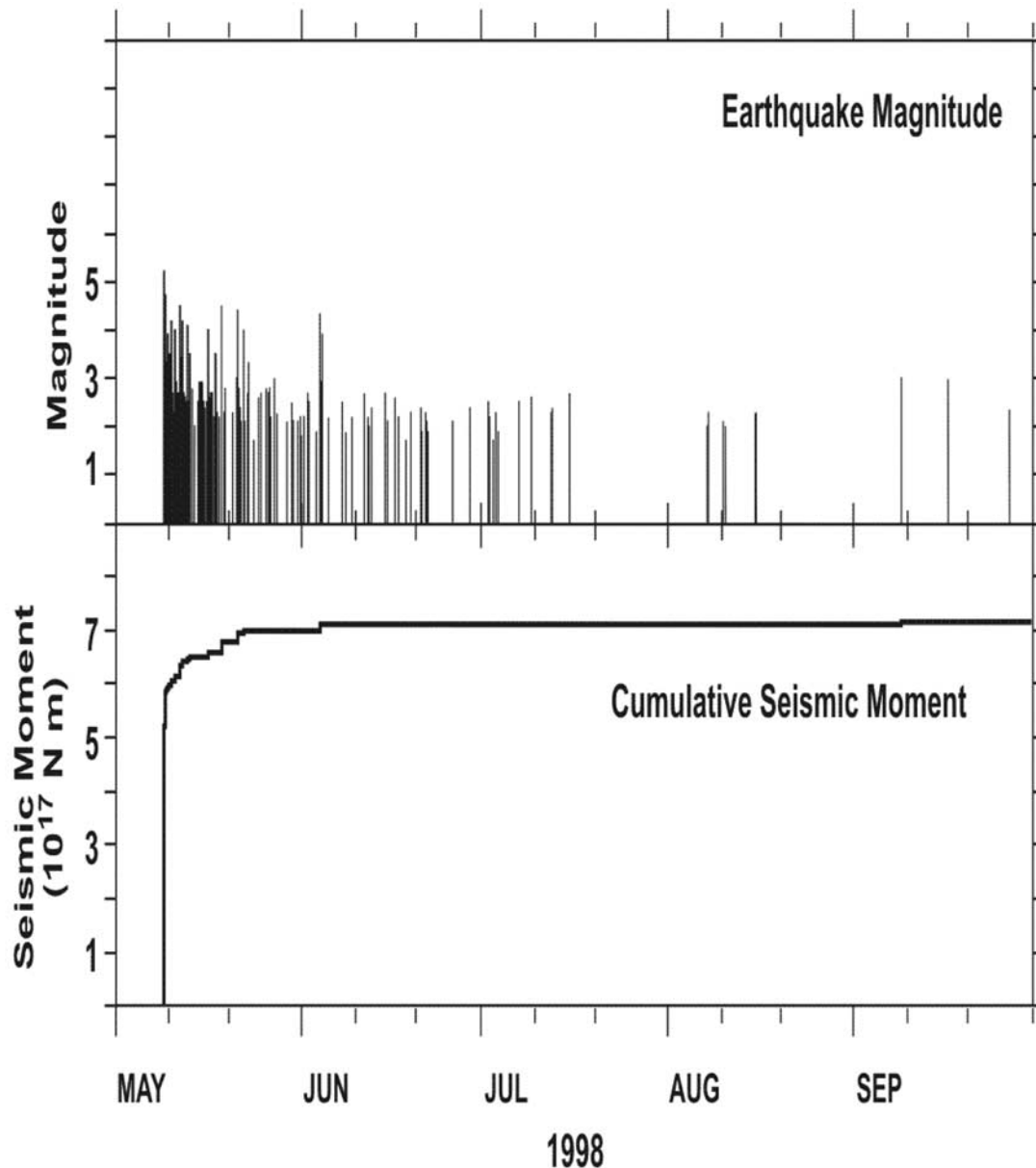
Figure 2. Time series plot showing earthquake magnitudes and cumulative seismic moment for the 1998 Becharof Lake earthquake swarm. Data provided by AVO.

The calculated depths for most of the swarm events are <7 km, but depth control is poor owing to the large distance to the nearest seismometer. Two temporary seismic stations deployed near Becharof Lake on 14–16 May (Figure 1) recorded 18 of these events, but relocations with and without data from the temporary stations resulted in only minimal movement (2.4 km epicentral and 2.9 km hypocentral, on average), indicating that most or all events in this sequence were, in fact, shallow and that the epicenters are generally correct. However, location errors might be largely responsible for the diffuse pattern of epicenters in Figure 1.

2. Radar Observations and Modeling Results

[10] We used the two-pass InSAR method [*Massonnet and Feigl*, 1998] with images acquired by the European Space Agency's (ESA) ERS-1 and ERS-2 satellites (Table 1) and the U.S. Geological Survey's (USGS) 15-min Alaska digital elevation model (DEM). The DEM has a specified horizontal accuracy of ∼60 m and root-mean-square vertical error of ∼15 m. We first verified the large-scale accuracy of the DEM using a pair of radar images acquired on 17 August 1992 and 21 September 1992 (the minimum repeat interval for most ERS-1/ERS-2 observations is 35 days). The altitude of ambiguity, h_a, for this image pair is ∼22 m, which means that large-scale, systematic DEM errors of that magnitude would produce one spurious interferometric fringe in a topography-removed interferogram formed from these two images. No fringes were evident in the topography-removed interferogram, which had good interferometric coherence across most of the study area, even in high-relief areas

Table 1. Interferometric Data Acquisition Parameters[a]

Dates	Δt, days	h_a, m	Easting x, km	Northing y, km	Depth d, km	Volume Change ΔV, km³	Variance σ^2, mm²	Figure
4 Oct. 1995 to 9 Oct. 1997	735	279	15.35 ± 0.09	14.28 ± 0.10	6.47 ± 0.25	0.043 ± 0.002	31.31	3a
8 Oct. 1996 to 23 Sept. 1997	350	70	15.19 ± 0.07	14.38 ± 0.09	6.63 ± 0.21	0.039 ± 0.002	29.64	3b
26 June 1997 to 9 Oct. 1997	105	30	14.68 ± 0.29	15.12 ± 0.35	6.60 ± 0.98	0.018 ± 0.007	54.21	4a
23 Sept. 1997 to 4 Aug. 1998	315	220	14.78 ± 0.18	15.32 ± 0.18	6.41 ± 0.46	0.012 ± 0.004	16.43	4c
9 Oct. 1997 to 24 Sept. 1998	385	134	15.29 ± 0.19	16.05 ± 0.19	7.72 ± 0.49	0.013 ± 0.005	28.56	4d
17 Aug. 1992 to 21 Sept. 1992[b]	35	22						4b
13 July 1992 to 21 June 1995[c]	1073	750						
21 Sept. 1992 to 26 July 1995[c]	1073	900						
30 Aug. 1995 to 15 Aug. 1996[c]	351	970						
18 Sept. 1995 to 3 Sept. 1996[c]	351	163						
20 Aug. 1998 to 9 Sept. 1999[c]	385	85						
24 Sept. 1998 to 5 Aug. 1999[c]	350	121						
9 Sept. 1999 to 20 July 2000[c]	350	488						
5 Aug. 1999 to 24 Aug. 2000[c]	385	70						

[a] Best fitting model parameters and uncertainties estimated at 95% confidence level are presented for interferograms with deformation. Horizontal x and y locations are measured with respect to the southwest corner of the study area.
[b] Used to verify large-scale DEM accuracy.
[c] No deformation.

such as Mount Peulik. All the interferograms used for our deformation analysis have h_a values ranging from 70 m to 970 m, except one 105-day interferogram with h_a = 30 m (Table 1 and Figures 3 and 4). These interferograms are much less sensitive to errors in the DEM than the above mentioned 35-day interferogram. Therefore any topographic artifacts in our deformation interferograms are negligible.

[11] Our data reduction and modeling strategy was as follows. First, we generated interferograms with large values of h_a (minimizing sensitivity to topographic errors) and long time intervals between the two SAR images (more likelihood of capturing ground deformation). If fringes were observed that seemed to indicate ground deformation, we generated more interferograms with shorter time intervals to rule out atmospheric artifacts, to confirm the deformation, and to constrain its timing. Most of the deformation observations reported here were confirmed using independent interferograms generated from image pairs that span similar time intervals but were acquired from different satellite tracks.

[12] Second, we modeled the observed deformation patterns using a spherical point pressure source embedded in an elastic homogeneous half-space [*McCann and Wilts*, 1951; *Mogi*, 1958], which fit the observations remarkably well. The four parameters used to describe the point source are horizontal location (easting x, northing y), depth d, and volume change ΔV of a presumed magma body, which is calculated by assuming that the injected magma has the same elastic properties as the country rocks [*Delaney and McTigue*, 1994; *Johnson et al.*, 2000]. The point source approximation is valid if the size of the source dimension is much smaller than its depth. A limitation of the half-space formulation is the neglect of topographic effects. To account for topographic effects, we adopted a simple approach proposed by *Williams and Wadge* [1998], in which the elevation of the reference surface varies according to the elevation of each computation point in the model. In our model we introduced a linear term in both x and y directions to account for possible errors in

determination of satellite positions, which might not be completely compensated for during interferogram processing [*Massonnet and Feigl*, 1998]. We used a nonlinear least squares inversion approach to optimize the source parameters [*Press et al.*, 1992]. The 95% confidence limits of the model parameters are estimated as follows. We first perturb one model parameter at a time. While holding that parameter fixed, we get the best fits for other model parameters by the nonlinear least squares inversion approach. We then use an F test to estimate the confidence limit of the perturbed parameter. The 95% confidence limits of model parameters are used to address the possibility of horizontal or vertical migration of the magma body during different time intervals. However, atmospheric anomalies may bias uncertainty estimations of model parameters. Because our models do not take into account any possible atmospheric delay anomalies in the deformation interferograms, the estimated significance of the difference between model parameters should be interpreted cautiously. Even if the atmospheric anomalies were absent in the interferograms, the confidence limits still depend on the validity of the source model and assumptions and on assumptions about the independence of the InSAR observations. To use the F test, we assume each modeled pixel in an interferogram is independent of the other pixels. This is not the case, but we currently do not know of a method to evaluate the dependence and use it in estimating more accurate confidence intervals. We leave that to future work.

2.1. No Significant Deformation From July 1992 to September 1996

[13] We generated four interferograms that collectively span the time interval from July 1992 to September 1996 (Table 1): (1) 13 July 1992 to 21 June 1995 (h_a = 750 m), (2) 21 September 1992 to 26 July 1995 (h_a = 900 m), (3) 30 August 1995 to 15 August 1996 (h_a = 970 m), and (4) 18 September 1995 to 3 September 1996 (h_a = 163 m). None of these interferograms included more than one recognizable fringe (2.83 cm of range change along the satellite look
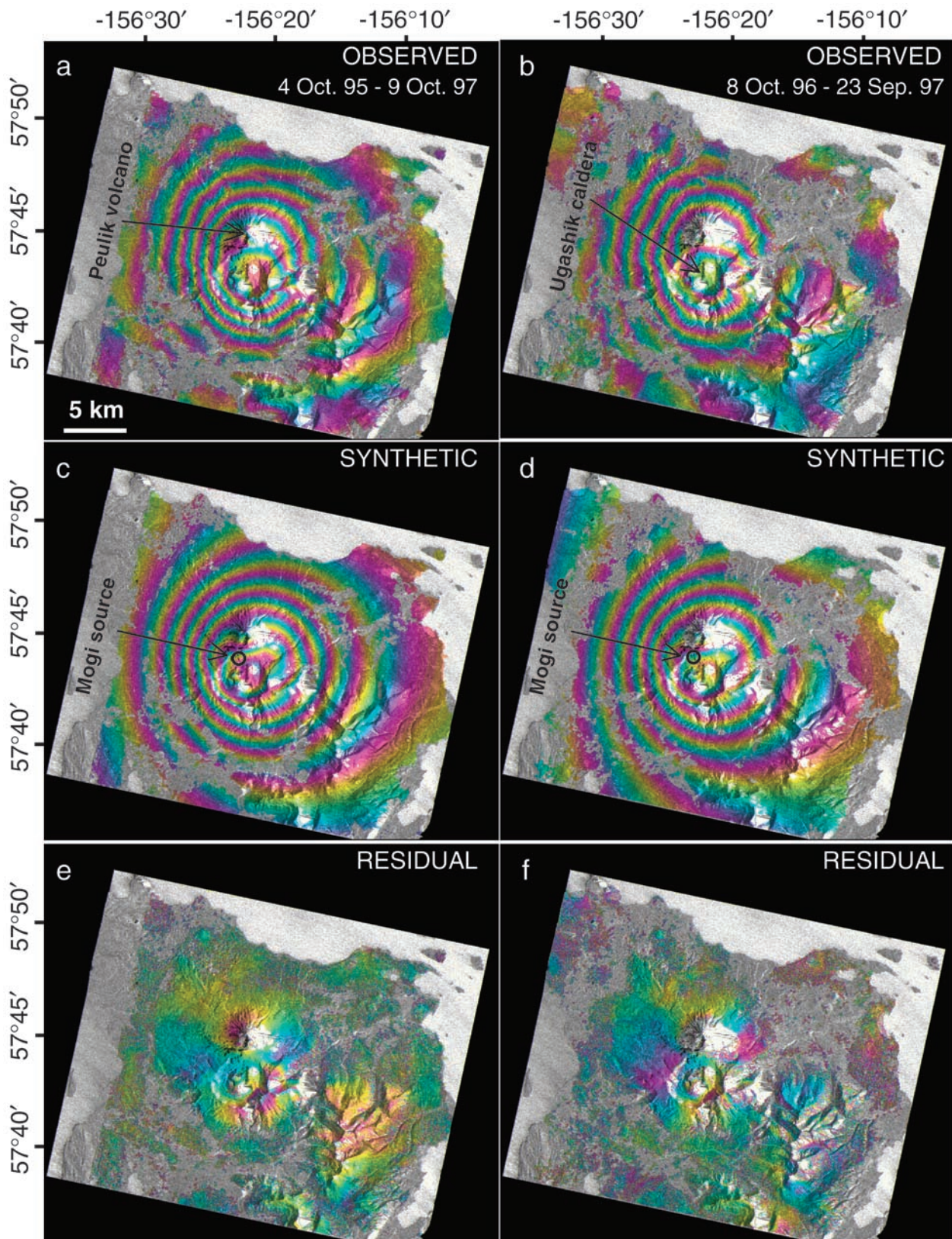
Figure 3. Topography-removed interferograms (observed, synthetic, and residual) for the Mount Peulik volcano. Each fringe (full color cycle) represents 2.83 cm of range change between the ground and the satellite. In this case, six concentric fringes represent ∼17 cm of uplift centered on the volcano's southwest flank. Synthetic interferograms were produced using a best fit inflationary point source at ∼6.5 km depth (circle in Figures 3c–3f), as discussed in the text. Areas of loss of radar coherence are uncolored.
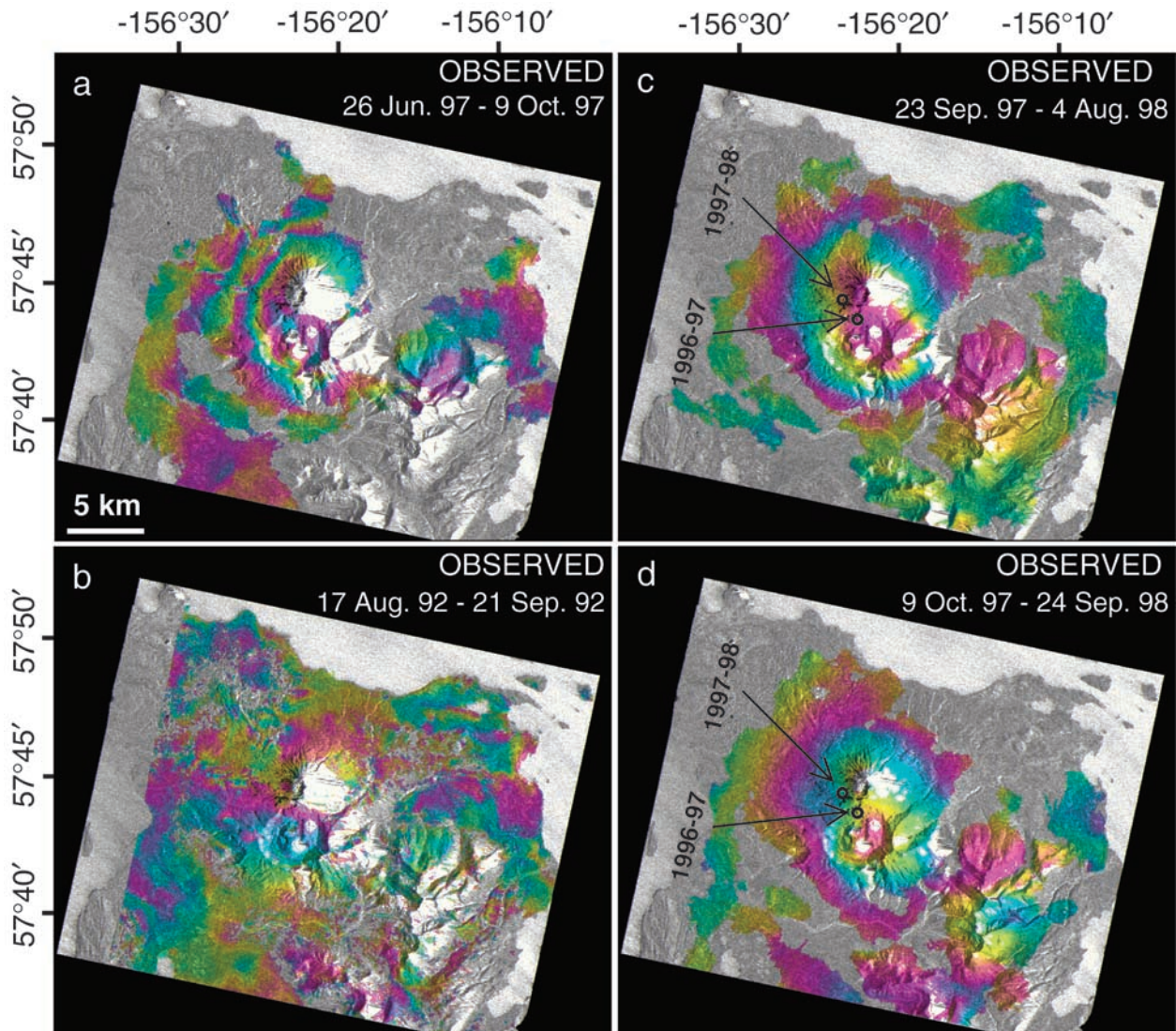
Figure 4. (a) Topography-removed interferogram for the period from 26 June to 9 October 1997, a period of relatively rapid inflation. (b) Topography-removed interferogram for the period from 17 August to 21 September 1992. The altitude of ambiguity for this interferogram is smaller than that for Figure 4a, indicating that most of the fringes in Figure 4a are not caused by errors in the DEM used. (c and d) Independent, topography-removed interferograms showing continued inflation during 1997–1998. Circles represent locations of best fit model sources, which shifted nearly 1 km northwestward from 1996–1997 to 1997–1998. Each fringe represents 2.83 cm of range change. Areas of loss of radar coherence are uncolored.

direction), and no consistent fringe pattern was discernible, so any ground deformation that might have occurred during that period was too small to measure.

2.2. Inflation of Mount Peulik Volcano From October 1996 to September 1997

[14] Figure 3a shows a deformation interferogram for the period from 4 October 1995 to 9 October 1997. As mentioned above, there was no deformation from July 1992 to September 1996, so the deformation recorded in Figure 3a must have occurred from October 1996 to October 1997. The value of h_a for the image pair is 279 m, so the interferogram is insensitive to any plausible errors in the DEM. The lack of strong correlation between

topography and fringe pattern and the redundancy of independent interferograms showing similar features discussed below argue strongly that the observed fringe pattern represents true ground deformation. More than six fringes are visible in the image (Figure 3a), which corresponds to ~17 cm of range shortening (i.e, surface uplift) along the satellite look direction. Maximum uplift occurs on the southwest flank of the Peulik volcano, near the center of the Ugashik caldera.

[15] We verified this result by forming an independent interferogram with images acquired on 8 October 1996 and 23 September 1997 ($h_a = 70$ m, Figure 3b). The image pairs used to form the interferograms in Figures 3a and 3b were acquired from two different satellite tracks. The

satellite look angle at the center of the images was ~23.6° for Figure 3a and 21.5° for Figure 3b. The fact that two interferograms formed from independent image pairs with very different altitudes of ambiguity showing essentially the same fringe pattern means that the fringes almost surely represent ground deformation that occurred between October 1996 and September 1997.

[16] Synthetic interferograms that correspond to the observed interferograms in Figures 3a and 3b are shown in Figures 3c and 3d, respectively. Model parameters and their uncertainties at the 95% confidence level are given in Table 1. All of the parameters are well constrained, mainly because the observed interferograms are coherent over most of the study area and the coherent pixels are distributed throughout the study area. The two models are essentially the same at the 95% confidence level. The model source is located beneath the southwest flank of the Mount Peulik volcano at a depth of 6.5 ± 0.2 km. The calculated volume change corresponding to Figures 3a and 3c is slightly larger than for Figures 3b and 3d (0.043 ± 0.002 km^3 versus 0.039 ± 0.002 km^3, respectively). The difference is not significant at the 95% confidence level.

[17] Most or all of the inflation described above occurred sometime between October 1996 and September 1997, but how long did the inflation episode last? Could it have been over in a matter of hours or days? To explore that possibility, we produced an interferogram that spans just 105 days, from 26 June 1997 to 9 October 1997. The value of h_a for this interferogram is only 30 m, so it is more sensitive to DEM errors than those in Figure 3a or 3b. Approximately two complete fringes centered at the Mount Peulik volcano are visible in the 105-day interferogram (Figure 4a). We concluded earlier that any large-scale errors in the DEM are less than ~22 m (Figure 4b), which corresponds to less than one fringe in the 105-day interferogram. Therefore we discount this possible source of error and attribute the fringe pattern in Figure 4a to inflation of the volcano. Our best fit model for the 105-day interferogram includes a volume change of 0.018 ± 0.007 km^3, which corresponds to an average inflation rate of 0.0051 ± 0.0020 km^3/month (Table 1). For comparison, the volume change during the 350-day interval from 8 October 1996 to 23 September 1997 was 0.043 ± 0.002 km^3, which corresponds to 0.0037 ± 0.0002 km^3/month. The average rates are similar, so the event spanned at least a few months and possibly more than a year. Inflation may have been relatively steady or episodic over that interval: Neither the InSAR results nor the absence of subvolcanic seismicity helps to distinguish between these possibilities.

[18] It appears from our modeling results that the deformation source might migrate nearly 1 km northwestward during 1996–1997 (compare northings and eastings for the first three models in Table 1). The variance of the best fitting model for the 105-day interferogram is nearly twice as large as the corresponding variances for the 735-day and 350-day interferograms (Figure 3), and the uncertainties in model parameters are also larger (Table 1). This is because the 105-day interferogram is noisier and not as fully coherent as the other two interferograms, as well as the fact that the 105-day interferogram is much more sensitive to any errors in the DEM. Nevertheless, if atmospheric delay anomalies are negligible, the difference between the

two model source locations is significant at the 95% confidence level. Although the amount of apparent source migration is small, its northwestward direction, toward the epicentral area of the Becharof Lake earthquake swarm, may be significant. The source depth, 6.6 ± 1.0 km, does not differ significantly from those obtained from the other modeling.

2.3. Continued Inflation From October 1997 to August 1998

[19] Two additional, independent interferograms clearly demonstrate that the Mount Peulik volcano continued to inflate after September 1997. The first interferogram spans the interval from 23 September 1997 to 4 August 1998 ($h_a = 220$ m), and the second spans the interval from 9 October 1997 to 24 September 1998 ($h_a = 134$ m). An apparent range change of slightly more than one fringe (2.83 cm) is visible in each of the interferograms (Figures 4c and 4d). Because the change is relatively small and the fringe "hugs" the topographic relief of the volcano, the fringe could be interpreted as a tropospheric delay anomaly [e.g., *Delacourt et al.*, 1998]. However, essentially the same fringe pattern occurs in two independent interferograms, and we did not observe any similar patterns in several short-term interferograms prior to 1995 (not shown here). Therefore we attribute the fringe patterns in the 1997–1998 interferograms to continuing inflation of the Mount Peulik volcano.

[20] Modeling the 1997–1998 interferograms yielded a depth for the point source that is similar to that for the three earlier interferograms (6–7 km, Table 1). The uncertainties in model parameters are larger for the 1997–1998 interferograms than for the 1995–1997 and 1996–1997 interferograms but smaller than those for the 105-day 1997 interferogram. The variance of the best fitting model derived from the first 1997–1998 interferogram (Figure 4c) is significantly smaller than for the second (Figure 4d), which suggests that the second interferogram might be contaminated by an atmospheric delay anomaly. The location of the deformation source in the first, more reliable model is consistent with our earlier conclusion that the source may have migrated northwestward during the course of the inflation episode (see Figures 4c and 4d).

2.4. No Significant Deformation From October 1998 to August 2000

[21] We generated four interferograms for this time period that span the following intervals (Table 1): (1) 20 August 1998 to 9 September 1999 ($h_a = 85$ m), (2) 24 September 1998 to 5 August 1999 ($h_a = 121$ m), (3) 9 September 1999 to 20 July 2000 ($h_a = 488$ m), and (4) 5 August 1999 to 24 August 2000 ($h_a = 70$ m). None of these interferograms revealed any significant deformation, so we conclude that the Peulik inflation episode ended sometime in 1998.

3. Discussion

[22] Although the 1996–1998 inflation episode at the Mount Peulik volcano and the 1998 earthquake swarm near Becharof Lake occurred in a remote area and did not

culminate in an eruption or a damaging earthquake, they are nonetheless important for scientific reasons. It has long been recognized that magmatic and tectonic processes are closely linked in many geologic settings, including active volcanic arcs such as the Aleutian arc. Many instances of apparent volcano-tectonic interactions have been reported in the literature, but no consistent theory to account for such interactions has yet been proposed. The most common type of report is either an eruption apparently triggered by a large earthquake or an earthquake (or earthquake swarm) apparently triggered by an eruption. The relative timing of the Mount Peulik inflation episode and Becharof Lake earthquake swarm suggests the latter relationship, except in this case the swarm may have been triggered by an intrusion that did not produce an eruption. If such an occurrence could be documented, it might shed new light on the significance of earthquakes near other arc volcanoes and provide an impetus to look for volcanic deformation whenever earthquakes occur nearby.

[23] Another reason that the Mount Peulik inflation episode is important is that it has implications for the eruption cycle at long-dormant stratovolcanoes and thus for hazard assessment and eruption forecasting. At arc volcanoes that seldom erupt, volcanologists have been mostly frustrated in their attempts to anticipate the beginning of new cycles of activity. Such volcanoes are quiescent for decades or centuries before unrest is recognized, typically a few days to months prior to eruptions. For example, the climactic 18 May 1980 eruption of Mount St. Helens was preceded by just 2 months of intense seismicity and flank deformation, a precursory period that represents ~0.1% of the 123-year repose interval since the end of the previous eruption. What happened beneath Mount St. Helens during the other 99.9% of its repose period? We believe that the 1996–1998 inflation episode at the Mount Peulik volcano provides some important insights in this regard, as discussed in section 3.2.

3.1. Stress Triggering of the Becharof Lake Earthquake Swarm?

[24] The relative timing of the Mount Peulik inflation episode (October 1996 to September 1998) and the 1998 Becharof Lake earthquake swarm (starting May 1998), as well as the fact that there was no clear main shock for the 1998 swarm, suggests that the swarm may have been triggered by a magmatic intrusion beneath the volcano. To evaluate this possibility, we calculated the Coulomb stress change caused by a volume increase of 0.05 km^3 in a point source located 6.5 km beneath the southwest flank of Mount Peulik. Guided by focal plane solutions for the two M_L 5.1–5.2 earthquakes, we calculated stress changes along vertical, left-lateral, N9°W striking faults at 6 km depth. Our results indicate that the epicenters of the two largest earthquakes and most of the smaller events are located in an area where the stress perturbation along NW trending faults was positive; that is, left-lateral strike slip was favored on these faults. However, the magnitude of the stress perturbation throughout the epicentral area is small, in the range 0.01–0.1 bar.

[25] Earthquake triggering by stress perturbations less than ~0.1 bar is considered unlikely because diurnal Earth tides produce stresses of up to 0.03 bar and do not generally trigger significant seismicity [Stein, 1999]. Nonetheless, the locations of the two largest swarm events and the preponderance of smaller events in an area of positive stress change suggest that magma intrusion beneath Peulik might have played a role in triggering the Becharof Lake earthquake swarm. Perhaps the 1996–1998 inflation episode was the latest in a series of events that cumulatively produced a stress perturbation large enough to trigger the 1998 swarm.

[26] The seismic activation of geologic structures at some distance from a restless volcano is not uncommon. Recent eruptions at Mount Pinatubo (Philippines) [Harlow et al., 1997], Montserrat (West Indies) [Aspinall et al., 1998], Guagua Pichincha (Ecuador) [Calahorrano, 2001], and Shishaldin (United States) [Moran et al., 2002] were all accompanied by earthquake activity at distances of 5–20 km from the vent. The 1977 and 1998 Becharof Lake earthquake swarms occurred in the same area, although the former accompanied the formation of the Ukinrek Maars (~15 km southeast of the epicentral area) and the latter accompanied inflation of Mount Peulik (~30 km southeast). The Ukinrek Maars magma is an alkali olivine basalt that does not seem to be linked geochemically to the Mount Peulik magmatic system [Kienle et al., 1980]. Nonetheless, the similarity of the 1977 and 1998 swarms suggests a connection of some sort between the Becharof Lake epicentral area, the Ukinrek Maars locality, and the Mount Peulik volcano.

[27] Other circumstantial evidence points to a possible link between Mount Peulik and the 1998 swarm. Our models indicate that the inflation center may have migrated nearly 1 km northwestward from 1996–1997 to 1997–1998. Although the shift is small, its direction suggests the possibility that magma moved laterally along a NW trending zone of weakness between Mount Peulik and the epicentral area. The existence of such a zone is suggested by the alignment of several vents in the area, including the summit of Mount Peulik, the vent for some recent lava flows on Mount Peulik's northwest flank, the Ukinrek Maars, and a littoral cone on the south shore of Becharof Lake (T. P. Miller, USGS, personal communication, 2000). The epicenters of the two M_L 5.1–5.2 earthquakes lie along a similar trend, as do a linear section of the Becharof Lake shoreline and a string of small lakes (Figure 5).

[28] Stauder [1968] identified a cross-arc tectonic boundary that seems to coincide with our hypothesized zone of weakness between Mount Peulik, the Ukinrek Maars, and the Becharof Lake epicentral area. He proposed that the Aleutian arc structure is segmented into distinct tectonic blocks with sharp boundaries that release their stored elastic strain independently in great earthquakes. One such boundary, according to Stauder [1968], is defined by the western extent of the aftershock zone of the 1964 Great Alaskan Earthquake (M_w = 9.2) and the eastern extent of the aftershock zone of the 1938 earthquake (M_w = 8.2) (Figure 5a). As noted by Kienle et al. [1980], such a boundary would pass through Mount Peulik and the Ukinrek Maars. Kienle et al. [1980] also pointed out a dramatic change in volcano spacing and alignment in the vicinity of the Ukinrek Maars and Mount Peulik: Chiginagak and Aniakchak volcanoes to
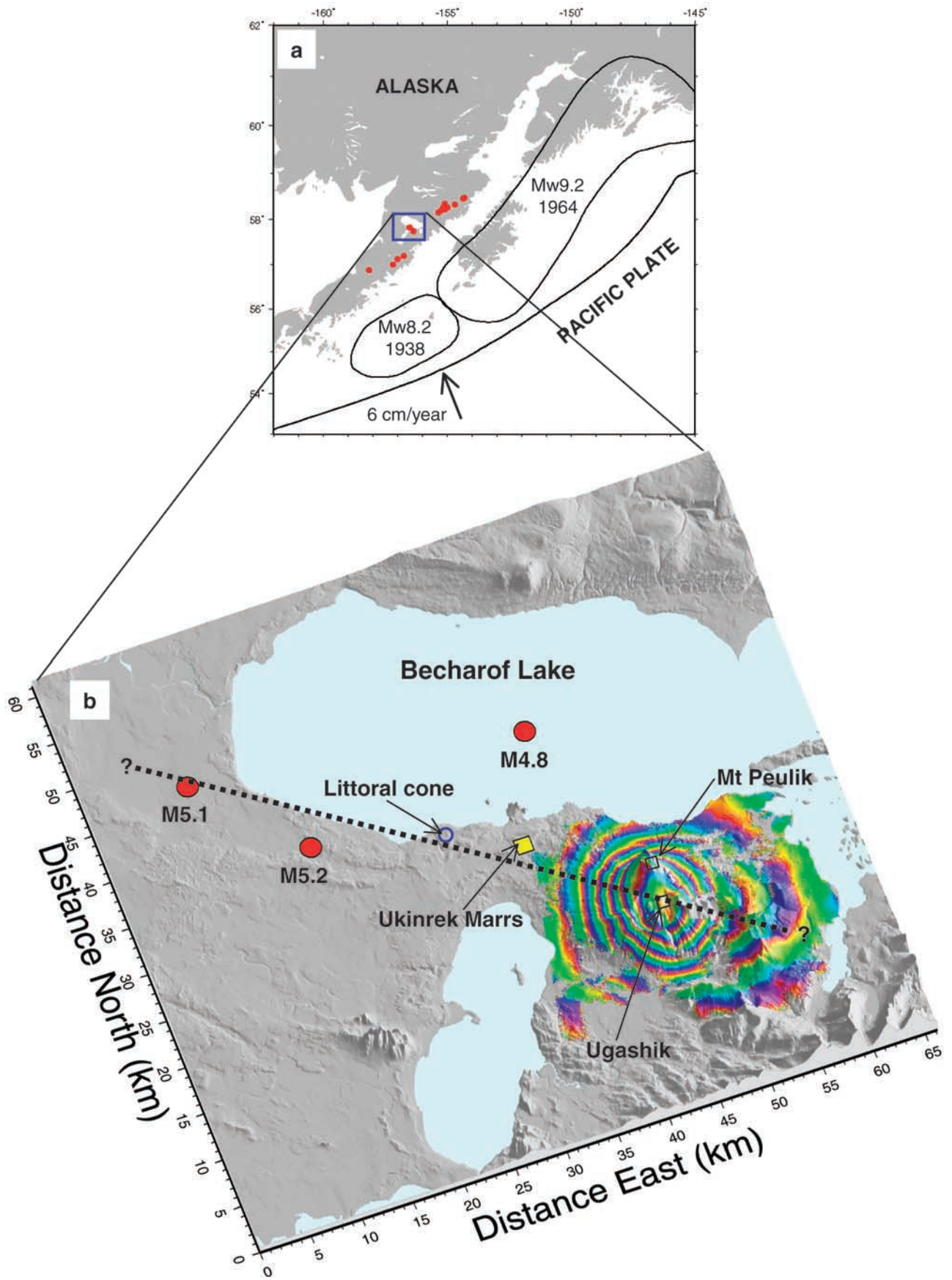
the west are clearly offset seaward from the Katmai volcano group to the east (Figure 5a).

3.2. Implications for the Eruption Cycle at Long-Dormant Stratovolcanoes

[29] Mostly aseismic deformation has also been detected with InSAR and other geodetic techniques at a few other magmatic systems that have not erupted for more than a century, including the Long Valley-Inyo-Mono system in eastcentral California and the Yellowstone system in northwest Wyoming. At Long Valley a period of episodic and sometimes intense unrest began with a *M* 5.7 earthquake near the Long Valley caldera on 4 October 1978. Subsequent activity during two decades has included numerous earthquake swarms beneath the caldera's south moat and nearby Mammoth Mountain, ~80 cm of uplift of the resurgent dome inside the caldera, changes in the shallow hydrothermal system, and increased emission of magmatic carbon dioxide in the vicinity of Mammoth Mountain. The area of maximum uplift on the resurgent dome has been virtually aseismic, apparently because the brittle-ductile transition in the crust is relatively shallow there and strain is released mainly by flow rather than brittle failure [*Hill et al.*, 1990; *Hill*, 1992, 1996]. The situation is similar at Yellowstone, where episodes of uplift and lesser subsidence are known to have occurred for several decades, accompanied by persistent and sometimes strong earthquake activity in the region but relatively little seismic energy release beneath the caldera itself [*Smith and Braile*, 1994; *Wicks et al.*, 1998].

[30] Aseismic inflation of Peulik differs from the Long Valley and Yellowstone cases in at least three significant respects. First, Peulik is a stratovolcano; Long Valley and Yellowstone are large silicic caldera systems. Conventional wisdom based on earlier monitoring experience holds that long-dormant stratovolcanoes deform mostly during brief periods of intense, shallow-seated unrest as magma intrudes the volcanic edifice and very little if at all during long periods between eruptions. Large calderas, on the other hand, commonly "breathe" (i.e., experience crustal uplift and subsidence) without producing eruptions and in some cases without any evidence of shallow intrusion. Second, the unrest at Long Valley and Yellowstone would have been noted even in the absence of geodetic measurements because nearby seismicity and hydrothermal changes were apparent. At Peulik, however, unrest would almost surely have escaped detection had it not been for InSAR. Finally, the discovery of aseismic inflation at Peulik hints at a richer eruption cycle at some stratovolcanoes than has commonly been assumed. Rather than lying entirely dormant for decades or centuries between eruptions before suddenly springing to life for a few months or years when magma intrudes the edifice, some stratovolcanoes may episodically approach eruption through a series of intrusions into the upper crust that can be detected geodetically. If so, tracking such events with InSAR may allow longer-term warnings of impending eruptive activity than have been possible in the past. Such warnings could be especially useful for long-term emergency preparedness and land use planning.

[31] The 1996–1998 inflation episode at the Mount Peulik volcano would almost surely have gone undetected if not for the occurrence of the Becharof Lake earthquake swarm, which was the impetus for our InSAR study of the area. Even though the 1998 epicenters are not well constrained, it is clear that most of the activity occurred 20–45 km northwest of Mount Peulik and few if any earthquakes occurred within 10 km of the volcano. This is an important finding because it suggests that aseismic inflation episodes may occur at other dormant stratovolcanoes as well. We suspect that such episodes are relatively common and an integral part of the eruption cycle. Many of these episodes may occur aseismically because magma accumulates gradually and preferentially near the brittle-ductile transition in the crust, which can be as shallow as ~5 km beneath active magmatic systems such as the Long Valley and Phlegraean Fields calderas [*Hill*, 1992]. Although shallow magma storage zones beneath stratovolcanoes are probably much smaller, episodic intrusions may in some cases heat the crust sufficiently to maintain a ductile zone within several kilometers of the surface. In such cases, inflation episodes will likely go undetected unless the intrusion rate is high enough to cause brittle failure or the regional stress field is such that a small amount of incremental stress is sufficient to trigger earthquakes along favorably oriented faults at some distance from the volcano.

[32] This is precisely what we suspect happened at Mount St. Helens, for example, for more than a century prior to its 1980 eruption. When, where, and how did the magma that erupted on 18 May 1980 accumulate beneath the volcano prior to its sudden invasion of the edifice in March 1980? *Scandone and Malone* [1985] showed that the hypocenters of well-located earthquakes that occurred soon after the eruptions of 18 May, 25 May, and 12 June 1980 outline an aseismic magma source region 7–14 km beneath the volcano. This inference was supported by *Moran* [1994], who concluded from the spatial distribution of earthquakes and focal mechanisms, as well as stress field modeling, that a magma reservoir 6.5–10 km beneath the volcano repressurized during 1987–1992. *Rutherford et al.* [1985] came to a similar conclusion about the location of the source region from a very different starting point. By comparison to experimentally determined phase equilibria, they showed that the mineral assemblage in 18 May pumice equilibrated at a pressure corresponding to a depth of 7.2 ± 1 km (i.e., near the top of the aseismic zone described above).

Figure 5. (opposite) (a) Location of Becharof Lake-Mount Peulik in the eastern part of the Aleutian arc. Red circles represent volcanoes in the surrounding areas. Aftershock zones for 1938 and 1964 are also shown. (b) Perspective view of topography near the Mount Peulik volcano. Superimposed on the topography is an interferogram for the period from October 1996 to September 1997, showing ~17 cm of uplift centered beneath the volcano's southwest flank. Each interferometric fringe (full color cycle) represents 2.83 cm of range change between the ground and the satellite. The dotted line marks an apparent alignment of several features (see text). We speculate that the alignment may indicate a fault or zone of weakness that facilitates magmatic intrusions.

[33] The 18 May 1980 eruption was preceded by 2 months of intense seismicity, flank deformation, and phreatic explosions starting in March 1980. By that time, magma had clearly intruded the edifice from a deeper source, presumably a magma body below ~7 km depth. Even in hindsight, no clear precursors to the eruption prior to March 1980 have been recognized. We are left to surmise that at least 0.3 km^3 (dense rock equivalent) of juvenile magma (the volume erupted on 18 May) accumulated at depths of 7–14 km sometime between 1857 (the end of the last eruptive episode) and March 1980 without being noticed. This may have occurred rapidly prior to the 1980 eruption or during a series of inflation episodes similar to the 1996–1998 event at Mount Peulik. It is unclear how many inflation episodes might have occurred, or when, during the 123-year repose.

[34] In light of the Mount Peulik results, we suspect that the eruption cycle at Mount St. Helens and other dormant stratovolcanoes may be much more eventful than has previously been recognized. Such volcanoes may inflate episodically during long periods of apparent quiescence until some threshold is reached, which triggers magma's final ascent to the surface. If so, InSAR provides a valuable tool for tracking a volcano's progress from one eruption to the next and for identifying quiescent volcanoes that warrant careful monitoring. Ultimately, more widespread use of InSAR for volcano monitoring could lead to improved volcano hazard assessments and better eruption preparedness.

4. Conclusions

[35] We formed several repeat-pass interferograms of the Becharof Lake-Mount Peulik region using more than 30 ERS-1 and ERS-2 SAR images acquired from 1992 to 2000. Independent interferograms formed with images that were acquired on different dates but which span similar time intervals confirm that similar patterns of interferometric fringes record inflation of the Mount Peulik volcano and are not artifacts caused by atmospheric effects or errors in the DEM used in the analysis. Using multiple interferograms, we were able to narrow the time window associated with the inflation episode to ~2 years preceding and probably including the time of the May 1998 Becharof Lake earthquake swarm. Our models of the deformation field reveal that a presumed magma body located 6.6 ± 0.5 km beneath the southwest flank of the Mount Peulik volcano inflated 0.051 ± 0.005 km^3 between October 1996 and September 1998. The average inflation rate of the inferred magma body was about 0.003 km^3/month from October 1996 to September 1997 and 0.001 km^3/month from October 1997 to September 1998 and peaked at 0.005 km^3/month during 26 June to 9 October 1997. Our models also suggest the possible migration of magma northwestward, toward the Becharof Lake swarm, during the course of the inflation episode.

[36] The relative timing of the Peulik inflation episode and the Becharof Lake earthquake swarm, as well as the fact that there was no clear main shock for the 1998 swarm, suggests that the swarm might have been triggered by a magmatic intrusion beneath the volcano. However, calculated static stress changes beneath the epicentral area due to inflation of a point source beneath Mount Peulik appear too small to provide a causal link. Perhaps the 1996–1998 inflation episode was the latest in a series of events that cumulatively produced a stress perturbation large enough to trigger the 1998 swarm.

[37] The 1996–1998 inflation episode at Mount Peulik is important because (1) it confirms that satellite radar interferometry can detect magma accumulation beneath dormant volcanoes at least several months before other signs of unrest are apparent and perhaps years before an eventual eruption, (2) it includes a possible case of earthquake stress triggering by a magmatic intrusion that might otherwise have gone unnoticed, and (3) it represents a first step toward understanding the eruption cycle at Mount Peulik and other stratovolcanoes with characteristically long repose periods. Similar studies at other dormant volcanoes where magma might be accumulating episodically and in some cases aseismically could lead to improved eruption forecasting and hazards mitigation.

References

Amelung, F., S. Jonsson, H. Zebker, and P. Segall, Widespread uplift and 'trapdoor' faulting on Galapagos volcanoes observed with radar interferometry, *Nature*, *407*, 993–996, 2000.

Aspinall, W., A. Miller, L. Lynch, J. Latchman, R. Stewart, and J. Power, Soufriere Hills eruption, Montserrat, 1995–1997: Volcanic earthquake locations and fault plane solutions, *Geophys. Res. Lett.*, *25*, 3397–3400, 1998.

Calahorrano, A., Study of 1998–1999 Quito seismic swarm origin (in Spanish), M.S. thesis, 199 pp., Escuela Politecn. Nac., Quito, Ecuador, 2001.

Delacourt, C., P. Briole, and J. Achache, Tropospheric corrections of the SAR interferograms with strong topography: Application to Etna, *Geophys. Res. Lett.*, *25*, 2849–2852, 1998.

Delaney, P. T., and D. F. McTigue, Volume of magma accumulation or withdrawal estimated from surface uplift or subsidence, with application to the 1960 collapse of Kilauea volcano, *Bull. Volcanol.*, *56*, 417–424, 1994.

Doroshin, P., Some volcanoes, their eruptions, and earthquakes in the former Russian holdings in America: Zu St. Petersburg (in Russian), Zweite Ser., Funfter Rand, 25–44, 1870.

Estes, S., Seismotectonic studies of lower Cook Inlet, Kodiak Island and the Alaska Peninsula area of Alaska, M.S. thesis, 142 pp., Univ. of Alaska Fairbanks, Fairbanks, 1978.

Harlow, D., J. Power, E. Laguerta, G. Ambubuyog, R. White, and R. P. Hoblitt, Precursory seismicity and forecasting of the June 15, 1991, eruption of Mount Pinatubo, Philippines, in *Fire and Mud: Eruptions and Lahars of Mount Pinatubo, Philippines*, edited by C. Newhall and R. Punongbuyan, pp. 285–306, Univ. of Wash. Press, Seattle, 1997.

Hill, D. P., Temperatures at the base of the seismogenic crust beneath Long Valley Caldera, California, and the Phlegraean Fields Caldera, Italy, in *Volcanic Seismology, IAVCEI Proc. Volcanol. Ser.*, vol. 3, edited by P. Gasparini, R. Scarpa, and K. Aki, pp. 433–461, Springer-Verlag, New York, 1992.

Hill, D. P., Earthquakes and carbon dioxide beneath Mammoth Mountain, California, *Seismol. Res. Lett.*, *67*(1), 8–15, 1996.

Hill, D. P., et al., The 1989 earthquake swarm beneath Mammoth Mountain, California: An initial look at the 4 May through 30 September activity, *Bull. Seismol. Soc. Am.*, *80*, 325–339, 1990.

Johnson, D. J., F. Sigmundsson, and P. T. Delaney, Comment on "Volume of magma accumulation or withdrawal estimated from surface uplift or subsidence, with application to the 1960 collapse of Kilauea volcano" by P. T. Delay and D. F. McTigue, *Bull. Volcanol.*, *61*, 491–493, 2000.

Kienle, J., P. R. Kyle, S. Self, R. J. Motyka, and V. Lorenz, Ukinrek Maars, Alaska, I, April 1977 eruption sequence, petrology, and tectonic setting, *J. Volcanol. Geotherm. Res.*, *7*, 11–37, 1980.

Lu, Z., D. Mann, J. Freymueller, and D. Meyer, Synthetic aperture radar interferometry of Okmok volcano, Alaska: Radar observations, *J. Geophys. Res.*, *105*, 10,791–10,806, 2000a.

Lu, Z., C. Wicks, D. Dzurisin, W. Thatcher, J. Freymueller, S. McNutt, and D. Mann, Aseismic inflation of Westdahl volcano, Alaska, revealed by satellite radar interferometry, *Geophys. Res. Lett.*, *27*, 1567–1570, 2000b.

Lu, Z., C. Wicks, J. Power, and D. Dzurisin, Ground deformation associated with the March 1996 earthquake swarm at Akutan volcano, Alaska, revealed by satellite radar interferometry, *J. Geophys. Res.*, *105*, 21,483–21,496, 2000c.

Lu, Z., C. Wicks, D. Dzurisin, W. Thatcher, and J. Power, Studies of volcanoes of Alaska by satellite radar interferometry, paper presented at ERS-Envisat Symposium, Eur. Space Agency, Gothenburg, Sweden, 2000d.

Lu, Z., J. Power, V. McConnell, C. Wicks, and D. Dzurisin, Preeruptive inflation and surface interferometric coherence characteristics revealed by satellite radar interferometry at Makushin volcano, Alaska: 1993–2000, *J. Geophys. Res.*, *107*, 10.1029/2001JB000970, in press, 2002a.

Lu, Z., T. Masterlark, J. Power, D. Dzurisin, and C. Wicks, Subsidence at Kiska volcano, western Aleutians, detected by satellite radar interferometry, *Geophys. Res. Lett.*, *29*, 10.1029/2002GL01498, in press, 2002b.

McCann, G. D., and C. H. Wilts, A mathematical analysis of the subsidence in the Long Beach–San Pedro area, report, Calif. Inst. of Technol., Pasadena, 1951.

Massonnet, D., and K. Feigl, Radar interferometry and its application to changes in the Earth's surface, *Rev. Geophys.*, *36*, 441–500, 1998.

Massonnet, D., P. Briole, and A. Arnaud, Deflation of Mount Etna monitored by spaceborne radar interferometry, *Nature*, *375*, 567–570, 1995.

Miller, T. P., R. G. McGimsey, D. H. Richter, J. R. Riehle, C. J. Nye, M. E. Yount, and J. A. Dumoulin, Catalog of the historically active volcanoes of Alaska, *U.S. Geol. Surv. Open File*, 98–582, 1998.

Mogi, K., Relations between the eruptions of various volcanoes and the deformations of the ground surface around them, *Bull. Earthquake Res. Inst. Univ. Tokyo*, *36*, 99–134, 1958.

Montserrat Volcano Monitoring Team, The ongoing eruption in Montserrat, *Science*, *276*, 371–372, 1997.

Moran, S. C., Seismicity at Mount St. Helens, 1987–1992: Evidence for repressurization of an active magmatic system, *J. Geophys. Res.*, *99*, 4341–4354, 1994.

Moran, S. C., S. D. Stihler, and J. A. Power, A tectonic earthquake sequence preceding the April–May 1999 eruption of Shishaldin volcano, Alaska, *Bull. Volcanol.*, in press, 2002.

Newhall, C. G., and D. Dzurisin, Historical unrest at large calderas of the world, *U.S. Geol. Surv. Bull.*, *1855*, 1108 pp., 1988.

Press, W., S. Teukolsky, W. Vetterling, and B. Flannery, *Numerical Recipes in C: The Art of Scientific Computing*, 994 pp., Cambridge Univ. Press, New York, 1992.

Punongbayan, R. S., et al., Eruption hazard assessments and warnings, in *Fire and Mud: Eruptions and Lahars of Mount Pinatubo, Philippines*, edited by C. G. Newhall and R. S. Punongbayan, pp. 415–433, Univ. of Wash. Press, Seattle, 1996.

Rutherford, M. J., H. Sigurdsson, S. Carey, and A. Davis, The May 18, 1980, eruption of Mount St. Helens, 1, Melt composition and experimental phase equilibria, *J. Geophys. Res.*, *90*, 2929–2947, 1985.

Scandone, R., and S. D. Malone, Magma supply, magma discharge and readjustment of the feeding system of Mount St. Helens during 1980, *J. Volcanol. Geotherm. Res.*, *23*, 239–262, 1985.

Self, S., J. Kienle, and J.-P. Huot, Ukinrek Maars, Alaska, II, Deposits and formation of the 1977 craters, *J. Volcanol. Geotherm. Res.*, *7*, 39–65, 1980.

Sibson, R., Fault zone models: heat flow, and the depth distribution of seismicity in the continental crust of the United States, *Bull. Seismol. Soc. Am.*, *72*, 151–163, 1982.

Smith, R. B., and L. W. Braile, The Yellowstone hotspot, *J. Volcanol. Geotherm. Res.*, *61*, 121–187, 1994.

Stauder, W., Tensional character of earthquake foci beneath the Aleutian trench with relation to sear-floor spreading, *J. Geophys. Res.*, *73*, 7693–7701, 1968.

Stein, R. S., The role of stress transfer in earthquake occurrence, *Nature*, *402*, 605–609, 1999.

Stein, R. S., G. C. P. King, and J. Lin, Stress triggering of the 1994 $M = 6.7$ Northridge, California, earthquake by its predecessors, *Science*, *265*, 1432–1435, 1994.

Swanson, D. A., T. J. Casadevall, D. Dzurisin, S. D. Malone, C. G. Newhall, and C. S. Weaver, Predicting eruptions at Mount St. Helens, June 1980 through December 1982, *Science*, *221*, 1369–1376, 1983.

Thatcher, W., and D. Massonnet, Crustal deformation at Long Valley caldera, eastern California, 1992–1996, inferred from satellite radar interferometry, *Geophys. Res. Lett.*, *24*, 2519–2522, 1997.

Vadon, H., and F. Sigmundsson, Crustal deformation from 1992 to 1995 at the Mid-Atlantic Ridge, southwest Iceland, mapped by satellite radar interferometry, *Science*, *275*, 193–197, 1996.

Ward, P. L., A. M. Pitt, and E. Endo, Seismic evidence for magma in the vicinity of Mt. Katmai, Alaska, *Geophys. Res. Lett.*, *18*, 1537–1540, 1991.

Wessel, P., and W. Smith, New version of Generic Mapping Tools (GMT) released, *Eos Trans. AGU*, *76*(33), 329, 1995.

Wicks, C., W. Thatcher, and D. Dzurisin, Migration of fluids beneath Yellowstone Caldera inferred from satellite radar interferometry, *Science*, *282*, 458–462, 1998.

Williams, C. A., and G. Wadge, The effects of topography on magma chamber deformation models: Application to Mt. Etna and radar interferometry, *Geophys. Res. Lett.*, *25*, 1549–1552, 1998.

Zebker, H., F. Amelung, and S. Jonsson, Remote sensing of volcano surface and internal processing using radar interferometry, in *Remote Sensing of Active Volcanism, Geophys. Monogr. Ser.*, vol. 116, edited by P. Mouginis-Mark et al., pp. 179–205, AGU, Washington, D.C., 2000.

———————————

D. Dzurisin, U.S. Geological Survey, David A. Johnston Cascades Volcano Observatory, 1300 SE Cardinal Court, Building 10, Suite 100, Vancouver, WA 98683-9589, USA. (dzurisin@usgs.gov)

Z. Lu, U.S. Geological Survey, EROS Data Center, Raytheon ITSS, 47914 252nd Street, Sioux Falls, SD 57198, USA. (lu@usgs.gov)

S. C. Moran and J. A. Power, U.S. Geological Survey, Alaska Volcano Observatory, 4200 University Drive, Anchorage, Alaska 99508, USA. (smoran@usgs.gov; jpower@usgs.gov)

W. Thatcher and C. Wicks Jr., U.S. Geological Survey, 345 Middlefield Road MS 977, Menlo Park, CA 94025-3591, USA. (thatcher@usgs.gov; cwicks@usgs.gov)